Somatic p16INK4a Loss Accelerates Melanomagenesis

Open

Oncogene (2010) 29, 5809–5817

www.nature.com/onc

ORIGINAL ARTICLE

Somatic p16^{INK4a} loss accelerates melanomagenesis

KB Monahan[1], GI Rozenberg[1], J Krishnamurthy[1], SM Johnson[1], W Liu[1], MK Bradford[1], J Horner[2], RA DePinho[2] and NE Sharpless[1]

[1]*Departments of Medicine and Genetics, The Lineberger Comprehensive Cancer Center, The Center for Environmental Health and Susceptibility, University of North Carolina School of Medicine, Chapel Hill, NC, USA and* [2]*Belfer Institute for Applied Cancer Science, Departments of Medical Oncology, Medicine and Genetics, Dana-Farber Cancer Institute, Harvard Medical School, Boston, MA, USA*

Loss of p16^{INK4a}–RB and ARF–p53 tumor suppressor pathways, as well as activation of RAS–RAF signaling, is seen in a majority of human melanomas. Although heterozygous germline mutations of *p16^{INK4a}* are associated with familial melanoma, most melanomas result from somatic genetic events: often p16^{INK4a} loss and N-RAS or B-RAF mutational activation, with a minority possessing alternative genetic alterations such as activating mutations in K-RAS and/or p53 inactivation. To generate a murine model of melanoma featuring some of these somatic genetic events, we engineered a novel conditional p16^{INK4a}-null allele and combined this allele with a melanocyte-specific, inducible CRE recombinase strain, a conditional p53-null allele and a loxP-stop-loxP activatable oncogenic K-Ras allele. We found potent synergy between melanocyte-specific activation of K-Ras and loss of p16^{INK4a} and/or p53 in melanomagenesis. Mice harboring melanocyte-specific activated K-Ras and loss of p16^{INK4a} and/or p53 developed invasive, unpigmented and nonmetastatic melanomas with short latency and high penetrance. In addition, the capacity of these somatic genetic events to rapidly induce melanomas in adult mice suggests that melanocytes remain susceptible to transformation throughout adulthood.
Oncogene (2010) **29,** 5809–5817; doi:10.1038/onc.2010.314; published online 9 August 2010

Keywords: melanoma; RAS; p16^{INK4a}

Introduction

Melanoma, the most lethal form of skin cancer, is increasing in incidence and mortality in the United States (Chin *et al*., 2006). Alterations of three genetic pathways characterize the majority of melanomas: activation of the RAS–RAF–extracellular signal-regulated kinase (ERK) pathway, inactivation of the p16^{INK4a}–CDK4–retinoblastoma (RB) pathway and inactivation of the alternate open reading frame (ARF)–murine double minute 2–p53 pathway. The RAS–RAF–ERK pathway is a mitogen-activated kinase cascade, which induces diverse transcriptional changes associated with increased proliferation, survival, motility and immune surveillance (Pearson *et al*., 2000; Johansson *et al*., 2007; Petermann *et al*., 2007; Shields *et al*., 2007). Per the Compilation of Somatic Mutations in Cancer (COSMIC, see (Forbes *et al*., 2006)), activating mutations of N-RAS occur in 21% of melanomas, those of K-RAS in 2% and of B-RAF in 44%, and these lesions seem to be mutually exclusive, consistent with an epistatic relationship. The presence of activating B-RAF mutations in a high proportion of dysplastic nevi indicates that aberrant activation of the RAS–RAF pathway is not sufficient for tumorigenesis and that additional genetic lesions are required to effect malignant transformation (Davies *et al*., 2002). Strong RAS–RAF activation has been shown to induce p16^{INK4a} expression and 'oncogene-induced senescence' *in vitro* and *in vivo* (Serrano *et al*., 1997; Zhu *et al*., 1998; Michaloglou *et al*., 2005), providing a tumor biological basis for cooperative interactions between p16^{INK4a} extinction and RAS–RAF activation.

The *INK4*/*ARF* (*CDKN2a*/*b*) locus at 9p21 encodes three distinct tumor suppressor proteins—p15^{INK4b}, p16^{INK4a} and ARF. A significant body of human and murine genetic data have determined that p16^{INK4a} and ARF have an important role in melanoma suppression (reviewed in (Kim and Sharpless, 2006)), whereas the role of p15^{INK4b} in this disease is less clear. *INK4a*/*ARF* deletion occurs in 50% of human melanomas, making it the most common site of genomic loss in melanomas (Curtin *et al*., 2005), with homozygous deletion being relatively common (Grafstrom *et al*., 2005). ARF blocks murine double minute 2-induced degradation of p53, whereas p16^{INK4a} and p15^{INK4b} inhibit cyclin-dependent kinases 4 and 6 , leading to RB-hypophosphorylation and cell cycle arrest. Although ARF loss is the most common lesion of the ARF–murine double minute 2–p53 pathway in melanoma, mutational inactivation of p53 is observed in 10–30% of melanomas (Albino *et al*., 1994; Sparrow *et al*., 1995; Akslen *et al*., 1998; Zerp *et al*., 1999).

Several genetically engineered mouse models of melanoma using constitutively active and inducible transgenes and germline knockout alleles have studied

Correspondence: Dr NE Sharpless, The Lineberger Cancer Center, CB# 7295, Departments of Medicine and Genetics, The University of North Carolina School of Medicine, Mason farm road, Chapel Hill, NC 27599-7295, USA.
E-mail: nes@med.unc.edu
Received 15 March 2010; revised 11 June 2010; accepted 19 June 2010; published online 9 August 2010

the interaction of Ras activation and p16INK4a/Arf/p53 loss. Mice engineered with a constitutive, melanocyte-specific, mutant H-Ras transgenic allele on an *Ink4a/Arf*-deficient background (*TyrRas Ink4a/Arf* −/−) were shown to develop melanoma with high penetrance and short latency (Chin *et al*., 1997). Using a doxycycline-inducible mutant H-Ras allele on an *Ink4a/Arf*-deficient background, it was determined that persistent activation of H-Ras is required for both melanoma initiation and maintenance, thus establishing the concept of tumor maintenance (Chin *et al*., 1999). Melanocyte-specific expression of an activated N-Ras transgene in an *Ink4a/Arf*-deficient background can also generate melanomas that can metastasize to the lymph nodes, lung and liver (Ackermann *et al*., 2005). A role for p53 in melanoma was substantiated in *TyrRas* transgenic mice that were mutant for p53, which develop melanomas that retain strong p16INK4a expression (Bardeesy *et al*., 2001). It is noteworthy and of relevance to this study that the *TyrRas* transgene on a germline *p16INK4a*-null background exhibited a weaker melanoma phenotype when compared with the *TyrRas* transgene on either a germline *Arf* or *p53*-null background (Bardeesy *et al*., 2001; Kannan *et al*., 2003). This murine observation is curious in light of the prominent role of p16INK4a extinction in human melanomas, raising the possibility of cross-species differences in the rate-limiting role of this key RB pathway component and/or of the fact that germline vs somatic inactivation of p16INK4a is a critical parameter of its impact on melanocyte biology.

In aggregate, these genetic studies have clearly established the cooperation of Ras activation and Arf/p53 inactivation in melanomagenesis, but have suggested a more modest role for p16INK4a loss in driving melanoma development in the mouse. This modest impact of p16INK4a loss seems to contrast with the prominent role of p16INK4a in human melanoma, as reflected by the robust melanoma-prone condition in the setting of germline or somatic p16INK4a mutations that spare Arf or p15INK4b in many cases (FitzGerald *et al*., 1996; Smith-Sorensen and Hovig, 1996; Walker *et al*., 1998; Daniotti *et al*., 2004). It is important to note that a few cases of ARF germline or somatic mutations that spare p16INK4a have been identified, suggesting that both products of the *INK4a/ARF* locus have independent tumor suppressor activity in melanoma (Rizos *et al*., 2001; Hewitt *et al*., 2002). Several possible explanations for the apparent cross-species differences have been suggested, including differences in the anticancer potency of p16INK4a vs ARF between mouse and man (Gil and Peters, 2006; Evan and d'Adda di Fagagna, 2009), bias derived from studies using transgene-driven overexpression of activated Ras (Tuveson *et al*., 2004), as well as epigenetic compensation in mice germline null for p16INK4a. With regard to the latter possibility, germline p16INK4a inactivation is associated with increased, presumably compensatory, expression of other negative regulators of the cell cycle, such as p15INK4b and p18INK4c (Krimpenfort *et al*., 2007; Ramsey *et al*., 2007; Wiedemeyer *et al*., 2008). Furthermore, somatic loss of RB *in vitro* has been shown to transiently induce cell cycle entry that is later compensated by other RB-family proteins (Sage *et al*., 2003). Therefore, the apparent differences between human and murine melanoma with regard to tumor suppressor pathway inactivation could reflect technical features of the experimental model systems used or species differences between mouse and man.

Conditional activated knock-in and tetracycline-inducible alleles and conditional knockout alleles have enabled the study of somatic mutations in adult mice. The use of conditional strategies are particularly relevant to melanoma research, in which epidemiological studies have suggested that sun exposure during childhood may be more effective at inducing melanoma than sun exposure later in life (Bader *et al*., 1985; Harrison *et al*., 1994; English *et al*., 2005). In accordance with this view, Merlino and colleagues have shown that ultraviolet B treatment of *HGF/SF* transgenic mice effectively induces melanoma only in the neonatal period (3.5 days), but not in adult mice (Noonan *et al*., 2001). Similar results were noted in *TyrRas Arf*−/− mice, which also pointed to the p16INK4a–RB pathway as a key target of ultraviolet carcinogenic actions (Kannan *et al*., 2003). These results could indicate that ultraviolet B is less efficient at causing oncogenic mutations in adult mice, or that adult melanocytes are intrinsically more resistant to the transforming effects of oncogenic mutations. The latter model would be consistent with the notion of a 'developmental window' at young age during which melanocytes are more susceptible to transformation by a given set of oncogenic events.

Building on this previous history of melanoma modeling in mice, we used somatic and inducible alleles, including a newly engineered 'floxed' p16INK4a-specific null allele, to study the effects of somatic, melanocyte-specific loss of p16INK4a and/or p53 combined with somatic activation of an oncogenic K-Ras allele on melanomagenesis in neonatal and adult mice.

Results

To determine the effect of somatic loss of p16INK4a and/or p53 and activation of oncogenic K-Ras, we used an established 4-hydroxytamoxifen (4-OHT)-inducible melanocyte-specific CRE allele (*Tyr-CRE-ER^{T2}* (Bosenberg *et al*., 2006)), together with conditional alleles such as *Lox-Stop-Lox-KRas^{G12D}* (Johnson *et al*., 2001), a floxed p53-null allele (*p53^{L}* (Jonkers *et al*., 2001) and a newly generated floxed *p16INK4a*-null allele (*p16^{L}*). In a subset of mice, CRE recombination was confirmed using a β-galactosidase reporter allele that, on Cre-mediated excision of a Lox-Stop-Lox cassette, expresses the enzyme; it was observed that cells stain positively in the β-galactosidase assay (Rosa26-LSL-β-galactosidase, (Soriano, 1999)) (Supplementary Figure 1). The *p16^{L}* allele was generated by inserting LoxP elements ~3.5 kb 5′ to exon 1α and immediately 3′ to the *p16INK4a* exon 1α (Supplementary Figure 2a, see also Supplementary Methods). The 5′ LoxP element was placed in a variable

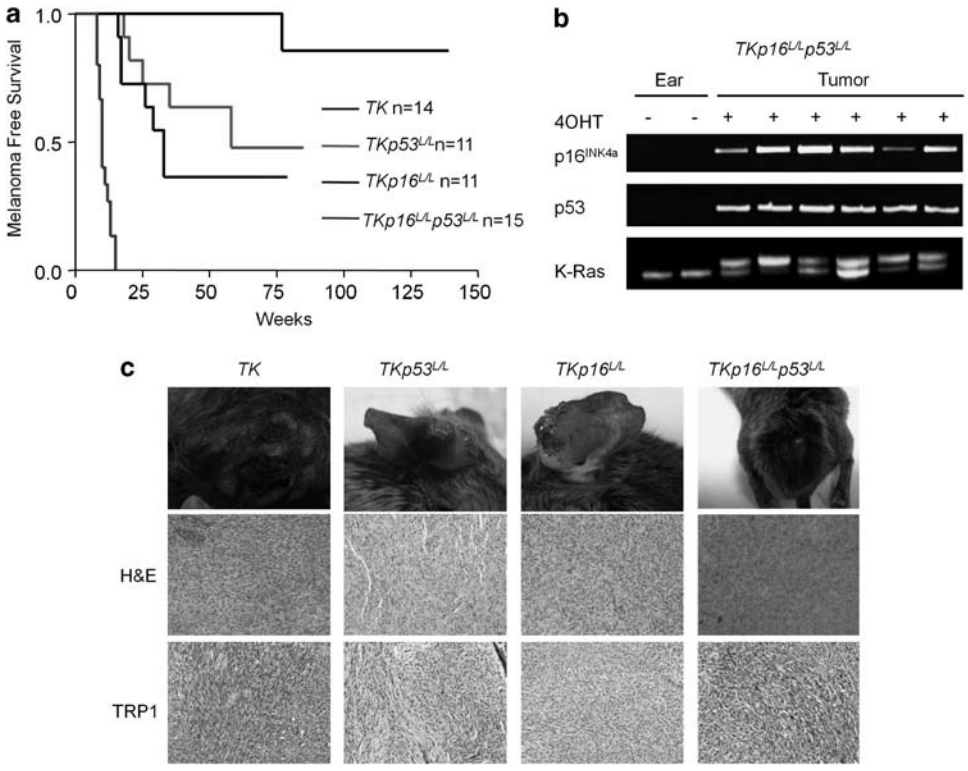

Figure 1 Somatic K-Ras activation coupled with $p16^{INK4a}$ and/or p53 inactivation induces melanoma. (**a**) Kaplan–Meier analysis of melanoma-free survival of 4-OHT-treated *TK* ($n=14$), $TKp16^{L/L}p53^{L/L}$ ($n=15$), $TKp16^{L/L}$ ($n=11$) and $TKp53^{L/L}$ ($n=11$) mice. Pairwise statistical comparisons: *TK* vs $TKp16^{L/L}$ ($P<0.001$), *TK* vs $TKp53^{L/L}$ ($P<0.001$), $TKp16^{L/L}p53^{L/L}$ vs $TKp16^{L/L}$ ($P<0.001$), $TKp16^{L/L}p53^{L/L}$ vs $TKp53^{L/L}$ ($P<0.001$) and $TKp16^{L/L}$ vs $TKp53^{L/L}$ ($P=$NS). (**b**) PCR for the recombined alleles: $K\text{-}Ras^{LSLG12D}$, $p16^{L/L}$, $p53^{L/L}$ in ears and tumors from 4-OHT-treated or untreated $TKp16^{L/L}p53^{L/L}$ mice. (**c**) Representative tumors from each cohort are shown. Tumors from mice of all genotypes exhibited a spindle-like morphology by hematoxylin and eosin staining and were stained for tyrosinase-related protein 1, confirming melanocytic origin. Original magnification: $\times 100$.

number of tandem repeat region that is not conserved between 129SvJ and C57Bl/6 strains, and therefore not likely to be a critical *Ink4a/Arf* regulator. Correct targeting of the locus was confirmed by Southern blotting, PCR and sequencing (Supplementary Figure 2b and c). CRE expression in $p16^{L/L}$ murine embryo fibroblasts and melanocytes demonstrated selective $p16^{INK4a}$ exon 1α excision, loss of $p16^{INK4a}$ protein expression (Supplementary Figure 3a and c) without an alteration in Arf expression (Supplementary Figure 3b and c). In contrast to deletion of Arf or p53, excision of $p16^{INK4a}$ with or without concomitant K-Ras activation did not enhance melanocyte growth *in vitro* (Supplementary Figure 3d).

Intercrosses produced the $Tyr\text{-}CRE\text{-}ER^{T2}+KRas^{LSL/+}p16^{L/L}p53^{L/L}$ experimental cohort ($TKp16^{L/L}p53^{L/L}$), as well as indicated control cohorts. $TKp16^{L/L}p53^{L/L}$ mice and control littermates were topically treated as neonates with 4-OHT to activate CRE and induce recombination in melanocytes as previously described (Bosenberg *et al*., 2006; see schematic in Supplementary Figure 1). Within 14 weeks, all 4-OHT-treated $TKp16^{L/L}p53^{L/L}$ mice developed aggressive tumors and hence had to be killed (Figure 1a, Table 1). Nonmelanoma tumors were not observed in 4-OHT-treated $TKp16^{L/L}p53^{L/L}$ mice ($n=15$) (Table 1). In contrast, only 1 of 14 of the 4-OHT-treated $TKp16^{+/+}p53^{+/+}$ mice developed melanoma at 60 weeks post treatment (Table 1). PCR confirmed that all $TKp16^{L/L}p53^{L/L}$ tumors exhibited a recombination of *K-Ras*, $p16^{INK4a}$ and *p53* alleles (Figure 1b). Western analysis of $TKp16^{L/L}p53^{L/L}$ tumors demonstrated an absence of expression of $p16^{INK4a}$ and p53, as well as of $p21^{CIP}$, a p53 target gene (Supplementary Figure 4a). These data demonstrate potent cooperation between activated K-Ras and combined $p16^{INK4a}$ and p53 loss in driving a highly penetrant and aggressive melanoma condition.

To further dissect the contributions of each tumor suppressor in melanoma development, we generated and compared $TKp16^{L/L}$ and $TKp53^{L/L}$ cohorts. These

Table 1 Summary of tumor features by genotype

Genotype	*Tumors/treated mice (%)*	*Median tumor latency*	*Metastasis*
TK	1/14 (7)	>52 weeks	None detected[a]
$Tp16^{L/L}p53^{L/L}$	1/19 (5)	>52 weeks	None detected
$TKp16^{L/L}$	8/11 (73)	24 weeks	None detected
$TKp53^{L/L}$	5/11 (45)	31 weeks	None detected
$TKp16^{L/+}p53^{L/+}$	3/7 (43)	>52 weeks	None detected
$TKp16^{L/L}p53^{L/L}$	15/15 (100)	9 weeks	None detected

[a]One lung tumor was noted in a 72-week-old animal of unclear histogenesis.

animals were treated neonatally by topical 4-OHT and followed up for tumor development, as outlined in Supplementary Figure 1. Somatic, melanocyte-specific loss of either p16^{INK4a} or p53 alone in this system led to melanoma formation (Figure 1a) with significantly longer tumor latencies than seen in the *TKp16$^{L/L}$p53$^{L/L}$* cohort but, notably, shorter than the latencies of the *TKp16$^{+/+}$p53$^{+/+}$* mice. Unexpectedly, the 4-OHT-treated *TKp16$^{L/L}$* and *TKp53$^{L/L}$* animals showed comparable median latencies of 24 and 31 weeks, respectively. The 4-OHT-treated compound heterozygous mice *TKp16$^{L/+}$* and *TKp53$^{L/+}$* showed accelerated tumorigenesis compared with 4-OHT-treated *TK* mice (Supplementary Figure 4b and Table 1). As expected, mice with somatic inactivation of p16^{INK4a} and p53 without concomitant Ras activation (*Tp16$^{L/L}$p53$^{L/L}$*) were only weakly tumor prone (1 of 19 mice, Table 1).

At the histopathological level, tumors from the four cohorts (*TK*, *TKp16$^{L/L}$*, *TKp53$^{L/L}$* and *TKp16$^{L/L}$p53$^{L/L}$*) exhibited a spindle-like morphology with scant pigmentation and positive staining for TRP1 (Figure 1c, Supplementary Figure 5). These 'amelanotic' melanomas are similar to those reported by Chin *et al*.(1997) in the H-Ras-driven *TyrRas Ink4a/Arf−/−* model, but different from the heavily pigmented tumors noted in N-Ras transgenic, *Ink4a/Arf*-deficient mice (Ackermann *et al*., 2005) and the conditional B-Raf and Pten mice (Dankort *et al*., 2009). In contrast to the *TyrRas Ink4a/Arf−/−* model, in which tumors are limited to ears, trunk, tail and uvea, tumors in the conditionally activatable model occurred on the flank, ear and tail, and uveal tumors were not observed. An increased tumor multiplicity was noted in 4-OHT-treated *TKp16$^{L/L}$ p53$^{L/L}$* mice compared with treated *TK*, *TKp16$^{L/L}$* or *TKp53$^{L/L}$* animals; however, there were significantly more tumors from treated *TKp16$^{L/L}$p53$^{L/L}$* mice when compared with *TK*, *TKp16$^{L/L}$* or *TKp53$^{L/L}$* animals, suggesting the increase in multiplicity could be due to an increase in the overall number of tumors (Supplementary Figure 4c). These data suggest that p16^{INK4a} and p53 exert important and nonredundant antimelanoma roles in the context of melanocyte-specific Ras activation, a finding that may reflect the prominent involvement of the *Ink4a/Arf* locus that dually encodes components of the RB and p53 pathway (Sherr, 2001).

Mice from all cohorts (*TK, TKp16$^{L/L}$*, *TKp53$^{L/L}$* and *TKp16$^{L/L}$p53$^{L/L}$*) developed melanocytic proliferation in the skin before tumor formation. Paws and tails of treated mice from all cohorts developed pigmented macules that were not present in wild-type or 4-OHT-untreated littermates (Supplementary Figure 6a and b). Wild-type and 4-OHT-untreated animals had little melanin production in sections of the ear when compared with treated mice from other cohorts. The most pronounced effects were observed in skin from 4-OHT-treated-*TKp16$^{L/L}$p53$^{L/L}$* mice (Supplementary Figure 6c). These findings suggest that K-Ras activation alone is sufficient to produce a modest increase in melanocytic proliferation, and that this excess, nonmalignant proliferation is partially restrained by the combined activities of p16^{INK4a} and p53.

To determine the role of the INK4–cyclin-dependent kinase 4 (Cdk4)–Rb pathway in melanocyte transformation *in vivo*, lysates of primary tumors were analyzed. In tumors from 4-OHT-treated mice of informative genotypes (*TKp53$^{L/L}$*, *TKp16$^{L/+}$p53$^{L/+}$and TKp16$^{L/+}$ p53$^{L/L}$*), the majority (8 of 11) of tumors demonstrated absent p16^{INK4a} expression (Figure 2a and b). Recently, expression of p15^{INK4b} has been shown to have a 'back-up' tumor suppressor role in p16^{INK4a} germline-deficient animals (Krimpenfort *et al*., 2007; Ramsey *et al*., 2007). In tumors from animals with somatic p16^{INK4a} and/or p53 inactivation, however, expression of p15^{INK4b} was observed in 8 of 12 tumors (Figure 2c). Therefore, any such compensatory increase in p15^{INK4b} expression either does not occur or is insufficient to prevent tumorigenesis in melanocytes in the setting of somatic deletion of p16^{INK4a}. In aggregate, these results imply that acquired stochastic loss of p16^{INK4a}, but not of p15^{INK4b}, is commonly associated with *in vivo* tumor progression in melanocytes harboring somatic, but not germline, p53 inactivation.

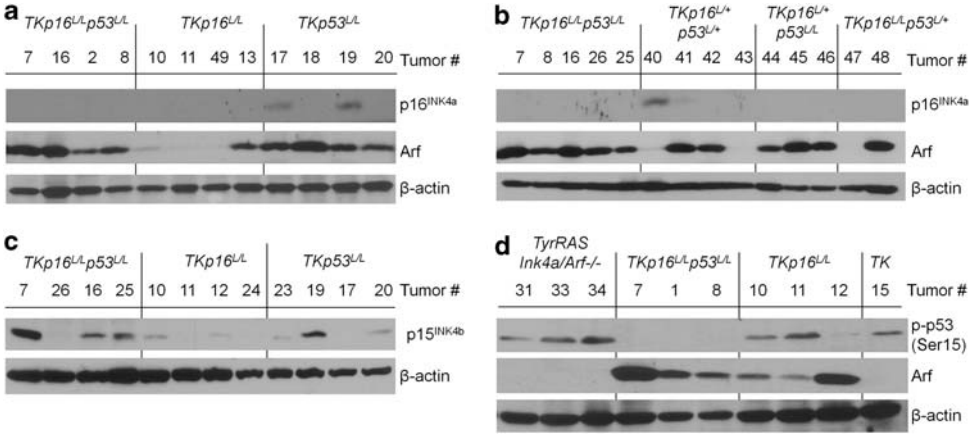

Figure 2 Analysis of INK4–Cdk4/6–Rb and Arf–p53 pathways in representative melanomas. (**a**) and (**b**) Western analysis of p16^{INK4a} and Arf in tumors of the indicated genotypes. (**c**) Western analysis of p15^{INK4b} expression in tumors of the indicated genotypes. (**d**) Western analysis of phospho-p53 and Arf in tumors of the indicated genotypes.

Similarly, we analyzed the Arf–p53 pathway in lysates from tumors from mice of informative genotypes. In accordance with previous reports (Chin *et al*., 1997; Bardeesy *et al*., 2001; Sharpless *et al*., 2002), we noted that tumors lacking p53 function almost always exhibited a markedly increased Arf expression (Figure 2b and d). As expected, tumors from contemporaneously analyzed *TyrRas Ink4a/Arf−/−* mice showed Arf loss and expression of phosphorylated p53 (Figure 2d). Analysis of $TKp16^{L/L}$ tumors demonstrated that four of five tumors exhibited phospho-p53 expression (Figure 2d), whereas three of five tumors exhibited Arf expression (Figure 2a and d). In particular, at least two $TKp16^{L/L}$ tumors (#10 and 11, Figure 2d) exhibited phospho-p53 and retained Arf expression, consistent with the possibility of a retained Arf–p53 pathway function in these tumors. In tumors from 4-OHT-treated mice that were heterozygous for the floxed p53 allele, absent Arf expression was noted in two of five tumors (Figure 2b), suggesting that Arf loss can be associated with tumor progression even in a $p53^{L/+}$ background. Although some $TKp16^{L/L}$ tumors retained Arf–p53 expression, other $TKp16^{L/L}$ tumors lost Arf expression, suggesting that Arf loss can contribute to progression in some tumors. Overall, these results suggest that somatic inactivation of the Arf–p53 pathway can occur, but is not obligate, for progression of K-Ras-induced, $p16^{INK4a}$-deficient melanoma.

In an effort to benchmark these new somatic models of melanoma to an earlier, well-characterized melanoma model, we also compared tumors from 4-OHT-treated $TKp16^{L/L}p53^{L/L}$ mice with contemporaneously analyzed *TyrRas Ink4a/Arf−/−* mice (Chin *et al*., 1997). It should be acknowledged that several relevant biological differences limit this comparison, including somatic vs germline genetic events; single copy, endogenous K-Ras mutation vs multicopy, transgenic H-Ras mutation; and p53 vs Arf loss. Although the tumor-inducing genetic events occur later (postnatally) in the $TKp16^{L/L}p53^{L/L}$ model, the tumor latencies were similar between the somatic and germline models (Figure 3a). Moreover, when the growth rates of comparably sized tumors were analyzed *in vivo*, melanomas from $TKp16^{L/L}p53^{L/L}$ mice were noted to grow more rapidly with increased ulceration (Figure 3b). All tumor-bearing $TKp16^{L/L}p53^{L/L}$ mice had to be killed by day 8 of observation because of advanced tumors, whereas *TyrRas Ink4a/Arf−/−* mice can routinely be observed for more than 20 days before having to be killed. Cell lines derived from $TKp16^{L/L}p53^{L/L}$ tumors demonstrated increased S-phase and aneuploidy compared with *TyrRas Ink4a/Arf−/−* tumors (Figure 3c, Supplementary Table 1). Consistent

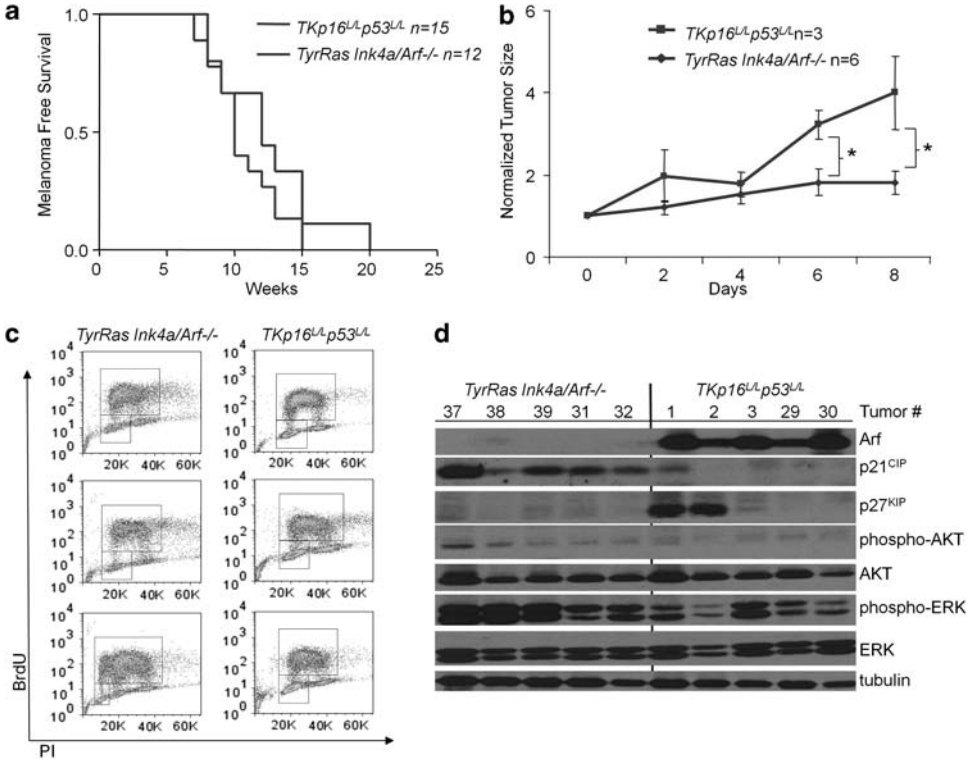

Figure 3 $TKp16^{L/L}p53^{L/L}$ melanomas are more aggressive than those from *TyrRas Ink4a/Arf−/−* mice. (**a**) Kaplan–Meier analysis of melanoma-free survival of $TKp16^{L/L}p53^{L/L}$ ($n=15$) and *TyrRas Ink4a/Arf−/−* ($n=12$) mice ($P=$NS). (**b**) *in vivo* analysis of tumor growth of $TKp16^{L/L}p53^{L/L}$ ($n=3$) and *TyrRas Ink4a/Arf−/−* ($n=6$) tumors. $^{*}P=0.01$ at days 6 and 8. (**c**) *in vitro* flow cytometry analysis of the cell cycle in tumor cell lines generated from $TKp16^{L/L}p53^{L/L}$ and *TyrRas Ink4a/Arf−/−* tumors. Increased S-phase and aneuploidy are noted in tumors from $TKp16^{L/L}p53^{L/L}$ mice (see also Supplementary Table 1). (**d**) Western analysis of indicated proteins in lysates from $TKp16^{L/L}p53^{L/L}$ and *TyrRas Ink4a/Arf−/−* tumors.

with loss of p53 vs Arf inactivation, Arf levels were increased and p21CIP levels decreased in $TKp16^{L/L}p53^{L/L}$ tumors compared with lines from *TyrRas Ink4a/Arf−/−* tumors (Figure 3d). Further characterization of protein expression in tumor lysates from the different models indicated little difference in the expression of tested downstream mediators of Ras signaling (for example, phospho-ERK and phospho-AKT, Figure 3d). These results are consistent with the possibility of a more aggressive *in vivo* behavior of $TKp16^{L/L}p53^{L/L}$ tumors as a result of p53 loss compared with Arf loss in the *TyrRas Ink4a/Arf−/−* model, although other differences such as strain background or Ras isoform differences could also contribute. Importantly, however, despite technical and biological differences between the models, they share several common features including tumor histological appearance, lack of precursor nevus formation, scant or absent tumor pigmentation and lack of metastasis. The shared features of Ras-driven, p16INK4a-deficient melanoma models are in contrast to the features of the pigmented, metastatic tumors seen in B-Raf mutant, Pten-deficient tumors reported by McMahon and Bosenberg (Dankort *et al*., 2009).

As epidemiological and murine modeling results have suggested that ultraviolet B exposure is more oncogenic at young ages, we studied the *in vivo* transformability of somatic K-Ras activation and combined p16INK4a/p53 loss in adult mice. Toward this end, small (1 cm × 1 cm) patches of flank skin were topically treated with 4-OHT in 8-week-old $TKp16^{L/L}p53^{L/L}$ mice and then manually depilated to stimulate melanocyte proliferation (see Supplementary Figure 1 and Ruzankina *et al*., 2007). By 15 weeks post 4-OHT treatment, tumor development was observed in the majority (17 out of 27) of treated $TKp16^{L/L}p53^{L/L}$ adult mice (Figure 4a and b), with all tumors developing at the site of 4-OHT treatment (Figure 4b and c). The median tumor latency of $TKp16^{L/L}p53^{L/L}$ mice was modestly longer in animals treated as adults compared with neonates (Figure 4a), but this may be explained by the considerably more extensive CRE-mediated recombination observed in neonatally treated mice (not shown, see also (Bosenberg *et al*., 2006)). To serially monitor melanoma development in adult mice, a green fluorescent protein CRE-reporter allele was crossed into the $TKp16^{L/L}p53^{L/L}$ model. Through intravital confocal microscopy of 4-OHT-treated $TKp16^{L/L}p53^{L/L}$ adult mice, CRE recombination was confirmed in 4-OHT-treated skin, but not noted in untreated skin (Figure 4c). Despite a basal level of autoflourescence in untreated skin, all $TKp16^{L/L}p53^{L/L}Rosa26\text{-}LSL\text{-}GFP+$ tumors expressed green fluorescent protein, allowing for visualization of individual tumor cells in anesthetized, living mice. These data are not consistent with the model of a 'developmental window' for melanocyte transformability, but instead show that adult melanocytes can be efficiently transformed *in vivo*.

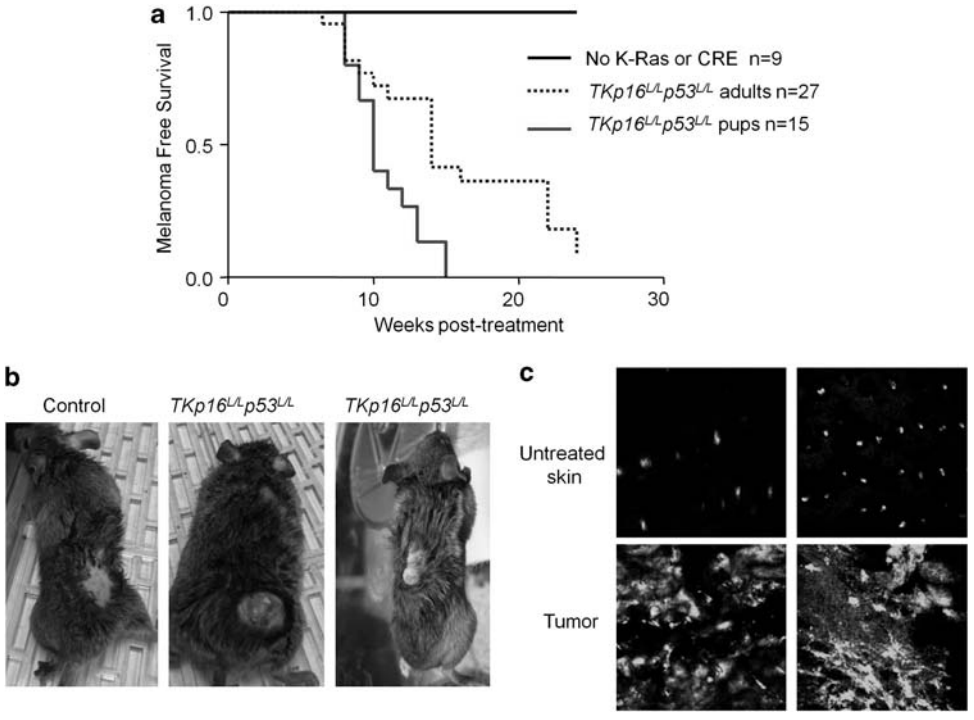

Figure 4 Melanocytes from adult $TKp16^{L/L}p53^{L/L}$ mice are transformable *in vivo*. (**a**) Kaplan–Meier analysis of melanoma survival of 4-OHT-treated $TKp16^{L/L}p53^{L/L}$ mice as adults or neonatal pups. Control mice (4-OHT-untreated or lacking the *K-Ras-LSL* allele ($n=9$)) did not develop tumors. Pairwise comparison of adult-treated ($n=27$) vs neonatally treated $TKp16^{L/L}p53^{L/L}$ mice ($n=15$) ($P=0.003$). (**b**) Adult $TKp16^{L/L}p53^{L/L}$ mice developed tumors in depilated and 4-OHT-treated skin patches. 4-OHT-treated control mice did not develop tumors. (**c**) Serial intravital confocal imaging of skin from $TKp16^{L/L}p53^{L/L}Rosa26\text{-}LSL\text{-}GFP+$ mice that were 4-OHT-treated as adults demonstrates green fluorescent protein expression and tumor growth. Melanocytes of untreated skin or of skin of control mice do not express green fluorescent protein; autoflourescence of hair follicles is noted. Original magnification: × 200.

Discussion

In this study, we provide evidence that somatic p16^{INK4a} deletion and oncogenic K-Ras activation promote the rapid onset of aggressive melanomas *in vivo*. To test somatic loss of p16^{INK4a} in melanoma, a novel p16^{INK4a} conditional allele was generated that exhibits unperturbed expression of other *Ink4a/Arf* locus genes, p15^{INK4b} and Arf. We observed potent cooperation between somatic Ras activation along with somatic p16^{INK4a} loss, whereas somatic Ras activation and p53 deletion yield a somewhat more modest melanoma-prone condition, a finding consistent the more prominent tumor suppressor role of p16^{INK4a} relative to p53 in human melanoma. These data support the view that conditional inactivation of p16^{INK4a} provides a more faithful platform for the generation of refined mouse models of human melanoma, and possibly of other cancers.

Moreover, as opposed to work using germline alleles (Kannan *et al*., 2003; Sharpless *et al*., 2003), the use of these conditional systems provides evidence that direct Arf-p53 inactivation is not required for *in vivo* murine melanoma formation. That is, some tumors arising in *TKp16$^{L/L}$* mice (Figure 4d) exhibited Arf and phospho-p53 expression. Although the analysis of *TKp16$^{L/L}$* tumors suggests that the ARF–p53 pathway retained expression, this does not eliminate other potential mechanisms that could abrogate the function of this pathway, such as point mutations or murine double minute 2 amplification. Nevertheless, although direct Arf or p53 inactivation does not seem to be an obligate event for *in vivo* melanomagenesis, our data and those of others certainly suggest that either lesion should strongly enhance tumor progression.

Although the primary tumors of *TKp16$^{L/L}$p53$^{L/L}$* mice were aggressive in terms of local invasion, we did not detect metastasis, a hallmark of human melanoma. Although metastasis has been observed in both an N-Ras transgenic model that used a multicopy transgene with a presumed high level Ras activation (Ackermann *et al*., 2005) and a somatic B-Raf mutant and Pten mouse model of melanoma (Dankort *et al*., 2009), metastasis has otherwise not been a feature of most murine melanoma models involving Ras activation, p53 loss and p16^{INK4a} loss (Chin *et al*., 1997; Bardeesy *et al*., 2001; Sharpless *et al*., 2003), suggesting that other factors are involved in metastasis in melanoma. One potential explanation could relate to Pten status, which is also inactivated with high frequency in human melanoma (reviewed in (Chin *et al*., 2006)). Several studies have suggested a prominent role for both the lipid and protein phosphatase activities of PTEN in regulating cellular motility and invasion (Tamura *et al*., 1998; Marino *et al*., 2002; Raftopoulou *et al*., 2004; Lin *et al*., 2009). Similar to other large tumor suppressor genes that can be inactivated by a variety of mechanisms, studies of PTEN in human cancer have been limited by difficulty in determining whether the gene is inactivated in a given tumor. Ongoing comprehensive studies such as the Cancer Genome Atlas involving multidimensional genome-scale analysis of large clinically annotated samples sets should determine whether PTEN loss is a primary driver of metastasis in human melanoma.

In summary, in this paper, we describe a genetically engineered murine model of melanoma that is based on somatic Ras activation and p16^{INK4a} loss, which are hallmarks of the human disease. This study has shown that somatic inactivation solely of p16^{INK4a}, without the corresponding targeting of Arf, is potently tumorigenic *in vivo*. Inactivation of p16^{INK4a} and p53 with Ras activation in adult melanocytes was potently oncogenic, suggesting that adult cells are not substantially less transformable than neonatal melanocytes. As novel targeted therapies for the RAS pathway are emerging for human melanoma (Engelman *et al*., 2008), these refined genetic models harboring genetic alterations encountered in the human disease should enable the more accurate use of such agents in specific melanoma genotypes in the future.

Materials and methods

Mouse colony

Animals were generated and genotyped as previously described (Johnson *et al*., 2001; Jonkers *et al*., 2001; Bosenberg *et al*., 2006) and were N1 in C57Bl/6. Mice were housed and treated in accordance with protocols approved by the institutional care and use committee for animal research at the University of North Carolina. Pups were treated for 3 consecutive days with 4-OHT (Sigma H7904, Sigma, St Louis, MO, USA) at 25 mg/ml in dimethyl sulfoxide starting at day 2 (Bosenberg *et al*., 2006). Tumor growth and survival were assessed three times per week by caliper measurements of tumor areas (width $\times$ length (mm^2)) and measurement was taken when tumors were between 20 and 30 mm^2. Tumor growth was normalized to day 1 values and analyzed using GraphPad Prism software (GraphPad Software, La Jolla, San Diego CA, USA).

Generation of p16$^{L/L}$ *allele and derivative cells*

The p16^{INK4a} conditional (floxed) allele (*p16^{L}*) was generated and validated as described in Supplementary Methods. To evaluate the effects of p16^{INK4a} excision, 1×10^6 murine embryonic fibroblasts were treated with CRE-expressing adenovirus (Iowa Vector Core, Iowa City, IA, USA) at a multiplicity of infection of 100 for 24 h. Cells were split and harvested 5 days after CRE treatment. To avoid the effects of adenoviral CRE expression on Arf–p53 expression, we crossed the *p16$^{L/L}$* allele into lentiviral transgenic CRE-ER^{T2} mice (Ruzankina *et al*., 2007). Murine embryo fibroblasts containing the CRE-ER^{T2} transgene and homozygous for the *p16$^{L/L}$* allele were generated and cultured on a 3T9 protocol. After four passages, cells were treated with 10 nm 4-OH-tamoxifen (Sigma T5648) for 40 h. After treatment, cell lysates were harvested at passages 1, 3 and 5. Primary melanocyte cultures from mice of the indicated genotypes, including the TyrCRE-ER^{T2} allele, were prepared as described previously (Bennett *et al*., 1989; Spanakis *et al*., 1992) and plated on collagen-coated dishes. Cells were treated with or without 4-OHT at 20 days post isolation for 48 h. Successful recombination was confirmed at 22 days and western blot was performed at 45 days. For growth curve analysis, cells were counted at indicated times and replated at 3×10^4 cells per ml. The mean relative population increase was calculated as the number of doublings.

Cell culture
Tumor cell lines were generated and maintained as described (Sharpless *et al*., 2002). For cell cycle analysis, exponentially growing cells were pulsed for 15 min with 10 μM bromodeoxyuridine (BrdU) in Dulbecco's modified Eagle's medium + 10% fetal calf serum before harvest. Cells were fixed, permabilized and stained with anti-BrdU-APC according to BrdU Flow Kit instructions (BD Pharmingen, San Jose, CA, USA) and then resuspended in phosphate-buffered saline + 0.2% fetal calf serum + 25 μg/ml propidium iodide with RNase and analyzed using a CyAn (Dako) flow cytometer (Cyan ADP, DAKO, Beckman Coulter, Brea, CA, USA) and FlowJo (Treesoft) software (Treestar, Inc., Ashland, OR, USA). Experiments were conducted in triplicate.

4-OHT treatment of adult mice and intravital microscopy
Hair on both flanks of 50- to 55-day-old mice was trimmed (1–2 cm^2 section) for treatment. One flank was treated with 20 mM 4-OHT dissolved in ethanol (treated skin) and the other flank was treated with 100% ethanol (control). Treatment was repeated the next day. Five days after treatment, mice were anesthetized with 2% isofluorane and depilated by hand (Ruzankina *et al*., 2007). For serial confocal imaging of tumors, mice were anesthetized with ketamine/xylazine and ear fur was removed using chemical depilation. Green fluorescent protein fluorescence in the ears was excited with 900-nm light from a Chameleon Ultra Ti-Sapphire pulsed laser (Coherent, Santa Clara, CA, USA) and imaged with a Zeiss LSM 510 NLO inverted 2-photon laser scanning microscope (Thornwood, NY, USA) using × 10 0.3 NA, × 20 0.5 NA and × 40 1.2 NA (water-immersion) objectives. Images were captured using a 12-bit cooled CCD camera (Hamamatsu, Bridgewater, NJ, USA).

Western blots
Western blot assays were performed on tumor lysates in RIPA buffer with protease inhibitors (Roche, Indianapolis, IN, USA) and phosphatase inhibitors (Calbiochem, EMD Chemicals Inc, Darmstadt, Germany) as described (Ramsey *et al*., 2007). Antibodies used were $p21^{CIP}$ (F-8, Santa Cruz, Santa Cruz, CA, USA), $p16^{INK4a}$ (M-156, Santa Cruz), β-actin (C-1, Santa Cruz), cyclin D1 (DCS-6, Cell Signaling, Danvers, MA, USA), cyclin E (M-20, Santa Cruz), Cdk2 (M2, Santa Cruz), Cdk4 (C-22, Santa Cruz), $p15^{INK4b}$ (K18, Santa Cruz), $p27^{KIP}$ (M20, Santa Cruz), phospho-p53 (Ser15, Cell Signaling), p53 (CM5, Novocastra Laboratories Ltd, Newcastle Upon Tyne, UK), p-ERK (9101S, Cell Signaling), ERK (9102, Cell Signaling), p-AKT (9271S, Cell Signaling), AKT (9272, Cell Signaling), Bax (Santa Cruz) and ARF (ab80, Abcam, Cambridge, MA, USA).

Immunohistochemistry
Assistance in sample processing was provided by the University of North Carolina Center for Gastrointestinal Biology and Disease. Ears and tumors were fixed in 10% formalin, paraffin-embedded, sectioned, deparaffinized and stained using hematoxylin and eosin for histological analysis. To confirm melanocytic origin, paraffin sections were treated with citric acid and stained with a rabbit anti-TRP1 (gift from Vincent Hearing) at a dilution of 1:500, or without primary antibody for control samples. Detection was performed using highly sensitive DAKO EnVision polymerized horseradish peroxidase. β-galactosidase staining was previously described (Bosenberg *et al*., 2006). Samples were analyzed (Zeiss Axioskop 2) and photographed (Zeiss Axiocam) under bright-field microscopy using × 10 0.25 NA, × 20 0.50 NA and × 40 1.30 NA objectives.

Statistical analysis
Tumor-free survival was analyzed using GraphPad Prism software (GraphPad Software) and comparisons were made using the log-rank test. Tumor sizes were compared using an unpaired, two-tailed *t*-test. Error bars ± s.e.m.

Conflict of interest

The authors declare no conflict of interest.

Acknowledgements

We thank Eric Brown, Marcus Bosenberg, Vincent Hearing for advice and reagents. This work was supported by Grants from NIH (AG024379 and ES14635), as well as from the American Federation of Aging (to KJ), the Golfers Against Cancer Foundation, the Sidney Kimmel Foundation and the National Cancer Center (to KBM).

References

Ackermann J, Frutschi M, Kaloulis K, McKee T, Trumpp A, Beermann F. (2005). Metastasizing melanoma formation caused by expression of activated N-RasQ61K on an INK4a-deficient background. *Cancer Res* **65**: 4005–4011.

Akslen LA, Monstad SE, Larsen B, Straume O, Ogreid D. (1998). Frequent mutations of the p53 gene in cutaneous melanoma of the nodular type. *Int J Cancer* **79**: 91–95.

Albino AP, Vidal MJ, McNutt NS, Shea CR, Prieto VG, Nanus DM *et al*. (1994). Mutation and expression of the p53 gene in human malignant melanoma. *Melanoma Res* **4**: 35–45.

Bader JL, Li FP, Olmstead PM, Strickman NA, Green DM. (1985). Childhood malignant melanoma. Incidence and etiology. *Am J Pediatr Hematol Oncol* **7**: 341–345.

Bardeesy N, Bastian BC, Hezel A, Pinkel D, DePinho RA, Chin L. (2001). Dual inactivation of RB and p53 pathways in RAS-induced melanomas. *Mol Cell Biol* **21**: 2144–2153.

Bennett DC, Cooper PJ, Dexter TJ, Devlin LM, Heasman J, Nester B. (1989). Cloned mouse melanocyte lines carrying the germline mutations albino and brown: complementation in culture. *Development* **105**: 379–385.

Bosenberg M, Muthusamy V, Curley DP, Wang Z, Hobbs C, Nelson B *et al*. (2006). Characterization of melanocyte-specific inducible Cre recombinase transgenic mice. *Genesis* **44**: 262–267.

Chin L, Garraway LA, Fisher DE. (2006). Malignant melanoma: genetics and therapeutics in the genomic era. *Genes Dev* **20**: 2149–2182.

Chin L, Pomerantz J, Polsky D, Jacobson M, Cohen C, Cordon-Cardo C *et al*. (1997). Cooperative effects of INK4a and ras in melanoma susceptibility *in vivo*. *Genes Dev* **11**: 2822–2834.

Chin L, Tam A, Pomerantz J, Wong M, Holash J, Bardeesy N *et al*. (1999). Essential role for oncogenic Ras in tumour maintenance. *Nature* **400**: 468–472.

Curtin JA, Fridlyand J, Kageshita T, Patel HN, Busam KJ, Kutzner H *et al*. (2005). Distinct sets of genetic alterations in melanoma. *N Engl J Med* **353**: 2135–2147.

Daniotti M, Oggionni M, Ranzani T, Vallacchi V, Campi V, Di Stasi D *et al*. (2004). BRAF alterations are associated with complex mutational profiles in malignant melanoma. *Oncogene* **23**: 5968–5977.

Dankort D, Curley DP, Cartlidge RA, Nelson B, Karnezis AN, Damsky Jr WE *et al*. (2009). Braf(V600E) cooperates with Pten loss to induce metastatic melanoma. *Nat Genet* **41**: 544–552.

Davies H, Bignell GR, Cox C, Stephens P, Edkins S, Clegg S *et al*. (2002). Mutations of the BRAF gene in human cancer. *Nature* **417**: 949–954.

Engelman JA, Chen L, Tan X, Crosby K, Guimaraes AR, Upadhyay R *et al*. (2008). Effective use of PI3K and MEK inhibitors to treat mutant Kras G12D and PIK3CA H1047R murine lung cancers. *Nat Med* **14**: 1351–1356.

English DR, Milne E, Simpson JA. (2005). Sun protection and the development of melanocytic nevi in children. *Cancer Epidemiol Biomarkers Prev* **14**: 2873–2876.

Evan GI, d'Adda di Fagagna F. (2009). Cellular senescence: hot or what? *Curr Opin Genet Dev* **19**: 25–31.

FitzGerald MG, Harkin DP, Silva-Arrieta S, MacDonald DJ, Lucchina LC, Unsal H *et al*. (1996). Prevalence of germ-line mutations in p16, p19ARF, and CDK4 in familial melanoma: analysis of a clinic-based population. *Proc Natl Acad Sci USA* **93**: 8541–8545.

Forbes S, Clements J, Dawson E, Bamford S, Webb T, Dogan A *et al*. (2006). COSMIC 2005. *Br J Cancer* **94**: 318–322.

Gil J, Peters G. (2006). Regulation of the INK4b-ARF-INK4a tumour suppressor locus: all for one or one for all. *Nat Rev Mol Cell Biol* **7**: 667–677.

Grafstrom E, Egyhazi S, Ringborg U, Hansson J, Platz A. (2005). Biallelic deletions in INK4 in cutaneous melanoma are common and associated with decreased survival. *Clin Cancer Res* **11**: 2991–2997.

Harrison SL, MacLennan R, Speare R, Wronski I. (1994). Sun exposure and melanocytic naevi in young Australian children. *Lancet* **344**: 1529–1532.

Hewitt C, Lee Wu C, Evans G, Howell A, Elles RG, Jordan R *et al*. (2002). Germline mutation of ARF in a melanoma kindred. *Hum Mol Genet* **11**: 1273–1279.

Johansson P, Pavey S, Hayward N. (2007). Confirmation of a BRAF mutation-associated gene expression signature in melanoma. *Pigment Cell Res* **20**: 216–221.

Johnson L, Mercer K, Greenbaum D, Bronson RT, Crowley D, Tuveson DA *et al*. (2001). Somatic activation of the K-ras oncogene causes early onset lung cancer in mice. *Nature* **410**: 1111–1116.

Jonkers J, Meuwissen R, van der Gulden H, Peterse H, van der Valk M, Berns A. (2001). Synergistic tumor suppressor activity of BRCA2 and p53 in a conditional mouse model for breast cancer. *Nat Genet* **29**: 418–425.

Kannan K, Sharpless NE, Xu J, O'Hagan RC, Bosenberg M, Chin L. (2003). Components of the Rb pathway are critical targets of UV mutagenesis in a murine melanoma model. *Proc Natl Acad Sci USA* **100**: 1221–1225.

Kim WY, Sharpless NE. (2006). The regulation of INK4/ARF in cancer and aging. *Cell* **127**: 265–275.

Krimpenfort P, Ijpenberg A, Song JY, van der Valk M, Nawijn M, Zevenhoven J *et al*. (2007). p15Ink4b is a critical tumour suppressor in the absence of p16Ink4a. *Nature* **448**: 943–946.

Lin HK, Wang G, Chen Z, Teruya-Feldstein J, Liu Y, Chan CH *et al*. (2009). Phosphorylation-dependent regulation of cytosolic localization and oncogenic function of Skp2 by Akt/PKB. *Nat Cell Biol* **11**: 420–432.

Marino S, Krimpenfort P, Leung C, van der Korput HA, Trapman J, Camenisch I *et al*. (2002). PTEN is essential for cell migration but not for fate determination and tumourigenesis in the cerebellum. *Development* **129**: 3513–3522.

Michaloglou C, Vredeveld LC, Soengas MS, Denoyelle C, Kuilman T, van der Horst CM *et al*. (2005). BRAFE600-associated senescence-like cell cycle arrest of human naevi. *Nature* **436**: 720–724.

Noonan FP, Recio JA, Takayama H, Duray P, Anver MR, Rush WL *et al*. (2001). Neonatal sunburn and melanoma in mice. *Nature* **413**: 271–272.

Pearson G, Bumeister R, Henry DO, Cobb MH, White MA. (2000). Uncoupling Raf1 from MEK1/2 impairs only a subset of cellular responses to Raf activation. *J Biol Chem* **275**: 37303–37306.

Petermann KB, Rozenberg GI, Zedek D, Groben P, McKinnon K, Buehler C *et al*. (2007). CD200 is induced by ERK and is a potential therapeutic target in melanoma. *J Clin Invest* **117**: 3922–3929.

Raftopoulou M, Etienne-Manneville S, Self A, Nicholls S, Hall A. (2004). Regulation of cell migration by the C2 domain of the tumor suppressor PTEN. *Science* **303**: 1179–1181.

Ramsey MR, Krishnamurthy J, Pei XH, Torrice C, Lin W, Carrasco DR *et al*. (2007). Expression of p16Ink4a compensates for p18Ink4c loss in cyclin-dependent kinase 4/6-dependent tumors and tissues. *Cancer Res* **67**: 4732–4741.

Rizos H, Puig S, Badenas C, Malvehy J, Darmanian AP, Jimenez L *et al*. (2001). A melanoma-associated germline mutation in exon 1beta inactivates p14ARF. *Oncogene* **20**: 5543–5547.

Ruzankina Y, Pinzon-Guzman C, Asare A, Ong T, Pontano L, Cotsarelis G *et al*. (2007). Deletion of the developmentally essential gene ATR in adult mice leads to age-related phenotypes and stem cell loss. *Cell Stem Cell* **1**: 113–126.

Sage J, Miller AL, Perez-Mancera PA, Wysocki JM, Jacks T. (2003). Acute mutation of retinoblastoma gene function is sufficient for cell cycle re-entry. *Nature* **424**: 223–228.

Serrano M, Lin AW, McCurrach ME, Beach D, Lowe SW. (1997). Oncogenic ras provokes premature cell senescence associated with accumulation of p53 and p16INK4a. *Cell* **88**: 593–602.

Sharpless NE, Alson S, Chan S, Silver DP, Castrillon DH, DePinho RA. (2002). p16(INK4a) and p53 deficiency cooperate in tumorigenesis. *Cancer Res* **62**: 2761–2765.

Sharpless NE, Kannan K, Xu J, Bosenberg MW, Chin L. (2003). Both products of the mouse Ink4a/Arf locus suppress melanoma formation *in vivo*. *Oncogene* **22**: 5055–5059.

Sherr CJ. (2001). The INK4a/ARF network in tumour suppression. *Nat Rev Mol Cell Biol* **2**: 731–737.

Shields JM, Thomas NE, Cregger M, Berger AJ, Leslie M, Torrice C *et al*. (2007). Lack of extracellular signal-regulated kinase mitogen-activated protein kinase signaling shows a new type of melanoma. *Cancer Res* **67**: 1502–1512.

Smith-Sorensen B, Hovig E. (1996). CDKN2A (p16INK4A) somatic and germline mutations. *Hum Mutat* **7**: 294–303.

Soriano P. (1999). Generalized lacZ expression with the ROSA26 Cre reporter strain. *Nat Genet* **21**: 70–71.

Spanakis E, Lamina P, Bennett DC. (1992). Effects of the developmental colour mutations silver and recessive spotting on proliferation of diploid and immortal mouse melanocytes in culture. *Development* **114**: 675–680.

Sparrow LE, Soong R, Dawkins HJ, Iacopetta BJ, Heenan PJ. (1995). p53 gene mutation and expression in naevi and melanomas. *Melanoma Res* **5**: 93–100.

Tamura M, Gu J, Matsumoto K, Aota S, Parsons R, Yamada KM. (1998). Inhibition of cell migration, spreading, and focal adhesions by tumor suppressor PTEN. *Science* **280**: 1614–1617.

Tuveson DA, Shaw AT, Willis NA, Silver DP, Jackson EL, Chang S *et al*. (2004). Endogenous oncogenic K-ras(G12D) stimulates proliferation and widespread neoplastic and developmental defects. *Cancer Cell* **5**: 375–387.

Walker GJ, Flores JF, Glendening JM, Lin AH, Markl ID, Fountain JW. (1998). Virtually 100% of melanoma cell lines harbor alterations at the DNA level within CDKN2A, CDKN2B, or one of their downstream targets. *Genes Chromosomes Cancer* **22**: 157–163.

Wiedemeyer R, Brennan C, Heffernan TP, Xiao Y, Mahoney J, Protopopov A *et al*. (2008). Feedback circuit among INK4 tumor suppressors constrains human glioblastoma development. *Cancer Cell* **13**: 355–364.

Zerp SF, van Elsas A, Peltenburg LT, Schrier PI. (1999). p53 mutations in human cutaneous melanoma correlate with sun exposure but are not always involved in melanomagenesis. *Br J Cancer* **79**: 921–926.

Zhu J, Woods D, McMahon M, Bishop JM. (1998). Senescence of human fibroblasts induced by oncogenic Raf. *Genes Dev* **12**: 2997–3007.

Supplementary Information accompanies the paper on the Oncogene website (http://www.nature.com/onc)